Odontology (2016) 104:357–362
DOI 10.1007/s10266-015-0228-z

ORIGINAL ARTICLE

Implant fracture under dynamic fatigue loading: influence of embedded angle and depth of implant

Hiroaki Suzuki[1] · Yoshiaki Hata[1] · Fumihiko Watanabe[1]

Received: 23 March 2015 / Accepted: 11 November 2015 / Published online: 23 December 2015
© The Society of The Nippon Dental University 2015

Abstract The purpose of this study was to investigate the relationship between implant fracture under cyclic-fatigue loading at different embedding angles, embedding depths, and loading forces. Twenty-four cylinder-type implants 3.3 mm in diameter and 10 mm in length were used. Test specimens were 30 mm^3 resin blocks with one surfaces inclined at angles of either 5°, 10°, 15° and 20° and embedded vertically with implants at depths of either 5 or 10 mm to the these surfaces. A straight abutment was connected to the implant and cut to 5 mm in length, and a hemispherical crown 5 mm in diameter and 7 mm in length was cast with a 12 % gold–silver–palladium alloy and cemented onto the abutment. Each specimen was mounted onto a fatigue loading device to apply repeated vertical loads of 294, 392, and 490 N to the coronal edge of the crown 60 times per min until reaching 100,000 cycles. For each respective specimen, we recorded the combined conditions of embedding and loading forces and the number of loading cycles until fracture, and then observed the fracture sites microscopically. The number of loading cycles until implant fracture tended to decrease in proportion to increased loading forces and embedded angles, and decreased embedded depths. Implant fracture was observed at angles of inclination over 10°. For specimens with an implant embedded at a depth of 5 mm, almost all fractures occurred at the center of the implant body; however, for those embedded at a depth of 10 mm, fractures occurred at the interface between the implant body and the abutment. These results demonstrate that implant fracture is associated with the loading axis, the amount of loading, and the embedded depth of the implant.

Keywords Implant fracture · Bending force · Loading angle · Implant axis · Cyclic-fatigue loading

Introduction

Although a majority of reports on implant-prosthetic restorations have presented a long-term predictable prognosis, some have focused attention on complications with abutment screw loosening, abutment screw fracture, implant component fracture, framework fracture, and loss of osseointegration [1–4]. Stress distribution in the implant body and superstructure has been suggested to be related to the following factors: implant position; embedded angle; embedded depth; loading angle with respect to the implant axis; fitness of superstructure with respect to the implant abutment; fitness of implant-abutment connection; and occlusal force [5–8].

In a two-stage implant system, the abutment is directly connected to the implant body using an abutment screw, and a superstructure is then fixed with a screw or cemented on it.

Within the oral cavity, level of bone support, loading axis with respect to the embedded implant, and amount of load may all act as triggers inducing implant, abutment, and abutment screw fracture. In particular, a restored crown on an obliquely embedded implant directly transmits a large amount of bending stress to both the implant body and surrounding bone, and repeated stress may promote fatigue failure of implant.

Although cyclic-fatigue loading tests have been conducted on implants in several studies to evaluate different

✉ Fumihiko Watanabe
fumi@ngt.ndu.ac.jp

[1] Department of Crown and Bridge Prosthodontics, The Nippon Dental University School of Life Dentistry at Niigata, Hamaura-chou 1-8, Chuuou-ku, Niigata 951-8580, Japan

dental implant systems [9, 10], relationships between fracture and loading conditions have not been discussed.

The fatigue loading fracture of the implant is considered to be caused by bending stress at the cycles of loading, loading direction, resorption of supporting bone and loading force.

Until now, these cause and effect of relationship has not been clarified clearly.

The purpose of this study was to investigate the relationship of implant fracture and a variety of factors, including embedded and loading angles with respect to the implant axis, embedded depth of the implant, and amount of load applied.

Materials and methods

Twenty-four cylinder-type implants (IMZ Twin Plus; Dentsply Friadent, Mannheim, Germany) 3.3 mm in diameter and 10 mm in length were used. For test specimens, 30-mm^3 resin blocks were prepared with one surface of each block having an inclined plane at angles of 5°, 10°, 15° or 20°. Holes measuring 3.3 mm in diameter and either 5 or 10 mm in depth were then vertically drilled at the center of each inclined surface using an IMZ Twin Plus drill (Dentsply Friadent). The implant body was secured into the prescribed depth using gentle tapping with a hammer and glued with cyano acrylate adhesive. An IMZ Twin Plus straight abutment (Dentsply Friadent) was connected to the implant by an abutment screw cut to 5 mm in length. A hemispherical crown 5 mm in diameter and 7 mm in length was directly waxed on the abutment and then cast with a 12 % gold–silver–palladium alloy (Castwell, GC Corp. Tokyo, Japan). The abutment was connected to the implant and the abutment screw was tightened to 20 N cm using torque ratchet (Dentsply Friadent). Zinc phosphate cement (Elite Cement, GC Corp) was mixed according to JIS [11] requirements. And the crown was cemented to the abutment using above cement under a 294 N vertical load to the implant axis for 24 h. The experimental conditions are provided in Table 1.

Table 1 Experimental conditions

	1	2	3	4
Embedded depth of implant (mm)	5	10		
Embedded angle of implant body (°)	5	10	15	20
Load				
(N)	294	392	490	
(kgf)	30	40	50	
Number of combinations = 2 × 4 × 3				

The specimen was fixed on the base of a servo-hydraulic machine (Servopulser EHF-FB; Shimadzu, Kyoto, Japan) for applying an impulsive load to the hemispherical crown according to ISO 14801 (Figs. 1, 2) [12]. Loads were repeated 100,000 times with 294, 392, or 490 N applied to the occlusal edge of the crown 60 times per min. Implants that fractured before completing 100,000 load cycles were recorded. A cross-section of each of the fractured sites was then observed visually with an optical microscope. All specimens were tested at random using a table of random numbers.

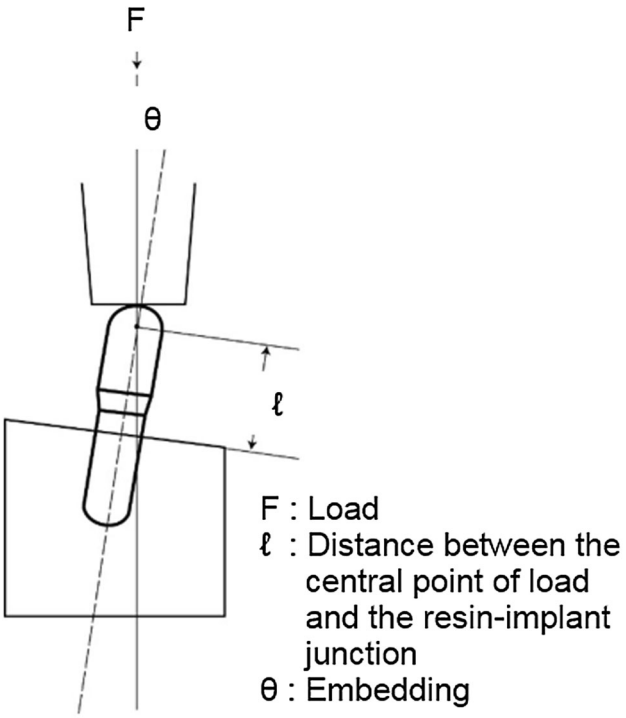

Fig. 1 Schematic of cyclic loading test

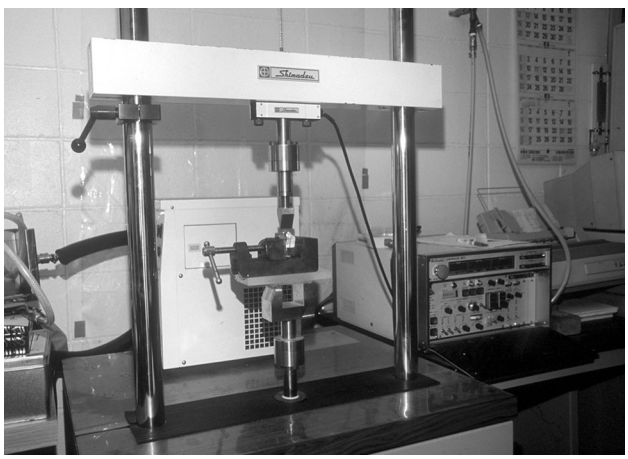

Fig. 2 Specimen fixed on the Servopulser

Table 2 Experimental results

Specimen No.	Embedded depth (mm)	Embedded angle (°)	Load (N)	Fracture and bending repeated numbers (times)	Bending moment (N cm)
1	5	5	294	–	33.3
2	5	5	392	–	44.4
3	5	5	490	–	55.5
4	5	10	294	–	66.3
5	5	10	392	57,650 Fracture of implant body	88.5
6	5	10	490	3,801 Fracture of implant body	110.6
7	5	15	294	–	98.9
8	5	15	392	28,024 Fracture at the connection of abut.	131.9
9	5	15	490	1,309 Fracture of implant body	164.9
10	5	20	294	12,156 Fracture of implant body	130.7
11	5	20	392	5,328 Fracture of implant body	174.3
12	5	20	490	36 Fracture of implant body	217.9
13	10	5	294	–	20.5
14	10	5	392	–	27.3
15	10	5	490	–	34.2
16	10	10	294	–	40.8
17	10	10	392	–	54.4
18	10	10	490	–	68.1
19	10	15	294	–	60.9
20	10	15	392	58,317 Fracture at the connection of abut	81.2
21	10	15	490	37,479 Fracture at the connection of abut	101.4
22	10	20	294	–	80.4
23	10	20	392	25,691 Fracture at the connection of abut	107.3
24	10	20	490	5,600 Fracture at the connection of abut	134.1

–, Not changed until 100,000 times

Results

Experimental data are presented in Table 2. The bending moment was also calculated. The maximum bending moment (M) for each specimen was calculated using the following formula: $M = \sin\theta \times \text{load} \times \text{distance}$ between the central point of load and the resin-implant junction (Fig. 1).

Fracturing or bending of the implant body or implant-abutment interface was largely influenced by the embedded depth. At 5 mm depth, fractures occurred at 10° or more under a loading force of 392 N or higher, while at 10 mm depth, fractures occurred at 15° or more under a force of 392 N or higher. The number of load cycles before fracture decreased with an increase in loading force (294, 392, and 490 N). At 5 mm depth, 15°, no changes were seen at 100,000 repetitions under 294 N loading; however, fracture did occur at the abutment-implant body interface at 28,000 repetitions under 392 N loading. Cross-sectional analysis showed that fracture site was the implant-abutment interface; its thin wall of implant was stretched and torn. These findings were common to all specimens with a fracture at the center of the implant body. At the implant-abutment interface, six projections of the abutment had interlocked with the inner grooves of the implant body, the compressed side of the implant wall was torn, and the grooves were deformed. A destruction fatigue testing is commonly shown graphically by the loading cycles, and the bending moment or maximum strength [13]. The relationship between number of fatigue loading cycles on each inclined degree and fracture of implant was indicated in Figs. 3 and 4

The S–N curve obtained from the cyclic load test is shown in Fig. 5. The dependent variable, fatigue life N in cycles, is plotted on the abscissa, a logarithmic scale.

Discussion

Experimental device

A cyclic-fatigue loading test was performed by repeatedly applying loads of 294, 392, and 490 N; these forces were comparable to the maximum human occlusal forces of

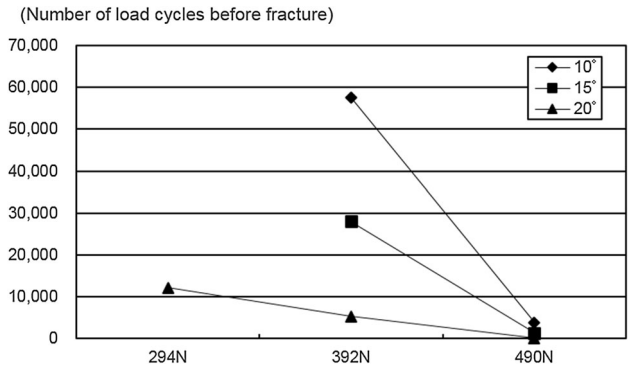

Fig. 3 Correlation emerged between the numbers of loading times and amount of loading to fracture in each loading angle

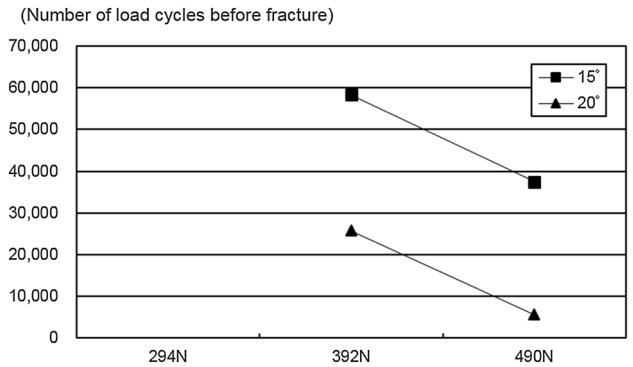

Fig. 4 Correlation emerged between the numbers of loading times and amount of loading to fracture in 15° and 20°

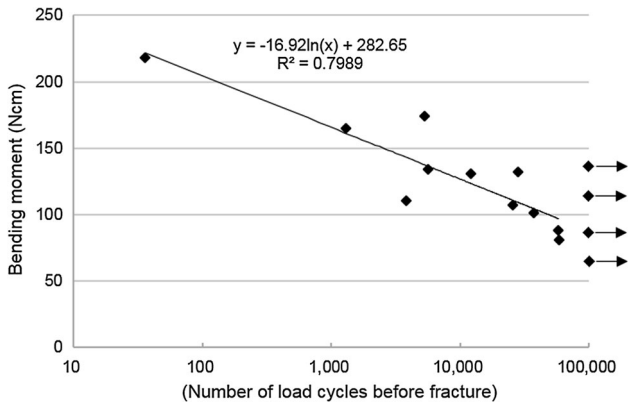

Fig. 5 Correlation emerged with the number of loading times to fracture

382.2 and 588 N for premolars and molars, respectively [14]. Although a certain degree of cushioning effect is provided in the human jaw, it is problematic to simulate it and excluded in experimental conditions, the implants in this experiment may have been subjected to more force than those in the human jaw. The hemispherical occlusal shape of the crown made it possible to apply a pulse load to each embedded implant body at the intended angle. Bending stress was correlated among all specimens, and therefore repeated trials were not considered necessary.

Load conditions

Based on the embedded implant angle, no fractures were found in the 5° specimens under loads of 294, 392, or 490 N. However, the 5 mm depth, 10° specimens were fractured at 57,600 times and 3800 times under loading forces of 392 and 490 N, respectively. No fractures occurred in 10 mm depth, 5° or 10 mm depth, 10° specimens under any loading conditions. The reason for this was that the distance from the resin-implant junction (fulcrum point) to the top (loading point) of the crown in 10 mm depth was smaller than that in 5 mm depth. As a result, in 5 mm depth, the bending moment was greater, and more stress was concentrated at the implant-abutment junction. Fractures occurred at 28,000 times in 5 mm depth, 15° specimens under a load of 392 N, and at 1310 times under a load of 490 N. On the other hand, fractures occurred at the implant-abutment junction at 58,300 and 37,500 times in 10 mm depth specimens under loads of 392 and 490 N, respectively. Therefore, an embedded implant angle of 15° appears to induce fracture. Implant-abutment fracture was also more likely with increases in the bending moment in proportion to the loading force.

Embedded angle of the implant

Embedded direction of the implant refers to the fatigue loading direction and the influence on fracture of the implant.

The bending moment of the implant body depends on the position of the fulcrum, and it is apparent that the bending moment increases with the increase of the embedded angle. These findings suggest that IMZ implants 3.3 mm in diameter and 10 mm in length will be fractured with an approximate 88.2 N cm bending moment.

Fatigue test of implant is carried out at varying loads and the number of load cycles, when the bending moment was investigated under various conditions, a correlation was evident with the number of loading times to fracture (Figs. 3, 4, 5). Specimens of 5 mm depth were not fractured at 5° under a maximum bending moment of 55.6 N cm; however, a bending moment of 88.2 N cm caused fracture of the implant body at 10° under a load of 39.2 N cm.

On observation of fractured implants, the site opposite to the bending point of the implant body was stretched and torn. More specifically, the number of loading times before fracture of the implant body tended to decrease with the increase of the embedded angle, and similarly, when load

force progressed to 490 N. For 10 depth specimens, no fracture occurred at 5° or 10°, but fracture was observed at the implant-abutment interface at 15° under a load of 392 N, and in this case, the bending strength was 81.3 N cm. The bending moment was higher for 20° than for 15° specimens, and the number of loading times to fracture decreased with the increase of the load force, provided that no fracture occurred under the 294 N load. The bending stress until fracture of the implant body used in this experiment appeared to be approximately 88.2 N cm, although this varied slightly depending on the experimental conditions. With-loading angles increase, the implant tends to fracture by less number of cyclic-fatigue loading.

Embedded depth of the implant

At 5 mm depth, fractures occurred at 10° loading while at 10 mm depth, fractures occurred at 15° loading. When 490 N loading was applied to 5 mm depth specimens, the bending moments were 55.9 N cm at 5°, 110.7 N cm at 10°, 164.6 N cm at 15° and 218.5 N cm at 20°. Shallow embedded implant is susceptible to fracture.

The implant embedded in 5 mm depth is fractured at 10° fatigue loading angle.

Goodacre et al. [15] reported when vertical bone loss coincides with the apical limit of the screw joining transepithelial abutment to implant, the risk of implant fracture increases considerably. In addition Green et al. [16] reported metal fatigue and bone resorption around implant were one of the causes of fracture.

Morgan et al. [17] analyzed fractured implants and concluded that commercially pure titanium implants failed due to bending fatigue. Rangert et al. [18] also concluded that the majority of fractures occurred in posterior quadrants where prostheses were prone to bending overload.

Huang et al. evaluated loading conditions on fatigue-failed implants and determined that there was a relationship between fracture surface morphology and the applied stress level for dental abutment screws under cyclic-fatigue loading. They demonstrated that the fracture surface analysis is a tool with great potential for assessing the mechanisms underlying fracture of dental implants [19]. They also pointed out that the loading angle is an important parameter in fracture analysis. Implant stress can be redistributed as a result of changes in the loading angle; therefore, specific relationships are thought to exist between loading angles and an implant's smooth and rough regions.

Dittmer et al. evaluated 6 different designs of implant-abutment assemblies (Astra, Bego, Camlog, Friadent, Nobel Biocare and Straumann) with respect to yield forces before and after cyclic-fatigue loading using a static overload test, with a test set-up according to ISO 14801. The results of this study suggest that conical implant-abutment connections may exhibit better continuity in yield forces over time [20].

Implant fracture was affected by the thickness of the implant wall when bending force was applied by cyclic loading. The IMZ Twin Plus 3.3 mm-diameter implants were accompanied by a wall thickness of 0.5 mm. Chan et al. reported that a specific implant wall thickness must be present to resist bending forces. The implant fractured when the thickness of the lateral walls became insufficient to resist the bending forces [21].

For connecting to the abutment, the upper section of the IMZ Twin Plus implant contains six notches for rotation-prevention, and the thin part of the wall, at a thickness of 0.5 mm, was associated with this mechanism. Therefore, at the embedding depth (support height) of 5 mm, loading stress concentrated at the center of the implant was associated with a thin wall. The repeated stress that fractured this part of the implant corresponded to the tip of the titanium screw connecting the abutment and the implant body. Thus, the edge of abutment screw acts as a fulcrum, and will fracture an implant body with a wall thickness of 0.5 mm.

The number of load cycles before fracture decreased with increasing load forces of 294, 392, and 490 N. This indicates that the higher the load force, the greater the repeated impulse forces on occlusion, and in turn, the greater the associated metal fatigue. Furthermore, fracture can easily occur when the embedded angle of the implant body exceeds 15° relative to the load direction. Accordingly, the angles formed by the lines of the embedded implant axis and the opposite tooth axis, should be assessed three-dimensionally. Even if it is impossible to avoid inclined embedding, an embedding angle of 5° or less is desirable, so as to transmit load force along the long axis of the implant body. As the specimens were directly fixed to the servo-hydraulic machine and subjected to repeated loads in this experiment, the load and stress applied to the implant bodies may be said to correspond roughly to the load and stress found in the oral cavity. The results of this study should provide further insight into the understanding of the use of dental implants in clinical practice.

Conclusion

The relationships between embedded depth, embedded angle, and cyclic loading until fracture or bending of an implant body were investigated. The results of the present study suggest that IMZ implants 3.3 mm in diameter and 10 mm in length will fracture with an approximate 88.2 N cm bending moment. Our results also suggest that

implant fracture is associated with the loading axis, the amount of loading, and the embedded depth of the implant in relation to the distance between the fulcrum and loading point of the prosthesis.

Compliance with ethical standards

Conflict of interest The authors are provided dental implants for the experiments from Dentsply Friadent. The authors declare that they have no other conflict of interest.

References

1. Jemt T. Failure and complications in 391 consecutive inserted fixed prostheses supported by Brånemark implants in edentulous jaws: a study of treatment from the time of prosthesis placement to the first annual checkup. Int J Oral Maxillofac Implants. 1991;6:270–6.
2. Lekholm U, Van Steenberghe D, Herrmann I, et al. Osseointegrated implants in the treatment of partially edentulous jaws: a prospective 5-year multicenter study. Int J Oral Maxillofac Implants. 1994;9:627–35.
3. Zarb GA, Schmitt A. The longitudinal clinical effectiveness of osseointegrated implants: the Toronto study. Part III: problems and complications encountered. J Prosthet Dent. 1990;64:185–94.
4. Goodacre CJ, Bernar G, Rungcharassaeng K, Kan JYK. Clinical complications with implants and implant prostheses. J Prosthet Dent. 2003;90:121–32.
5. Green NT, Machtei EE, Horwitz J, Peled M. Fracture of dental implants: literature review and report of a case. Implant Dent. 2002;11:137–43.
6. Balshi T. An analysis and management of fractured implants: a clinical report. Int J Oral Maxillofac Implants. 1996;11:660–6.
7. Schwarz MS. Mechanical complications of dental implants. Clin Oral Implants Res. 2000;11(Suppl 1):156–8.
8. Eckert SE, Meraw SJ, Cal E, Ow RK. Analysis of incidence and associated factors with fractured implants: a retrospective study. Int J Oral Maxillofac Implants. 2000;15:662–7.
9. Perriard J, Wiskott WA, Mellal A, Scherrer SS, Botsis J, Belser UC. Fatigue resistance of ITI implant-abutment connectors—a comparison of the standard cone with a novel internally keyed design. Clin Oral Implants Res. 2002;13:542–9.
10. Steinebrunner L, Wolfart S, Ludwig K, Kern M. Implant-abutment interface design affects fatigue and fracture strength of implants. Clin Oral Implants Res. 2008;19:1276–84.
11. Japan Industrial Standard. Zinc phosphate dental cement, T6602, 1993.
12. ISO 14801:2007. Dentistry—Implant—Dynamic fatigue test for endosseous dental implants.
13. ASTM E486-90:2004 Standard practice for presentation of constant amplitude fatigue test results for metallic materials.
14. Takamizawa T. Studies on the co-relative and individual biting forces of normal permanent teeth. J Jpn Prosthodont Soc. 1965;9:217–36.
15. Goodacre CJ, Kan JY, Rungcharassaeng K. Clinical complications of osseointegrated implants. J Prosthet Dent. 1999;81:537–52.
16. Green NT, Machtei EE, Horwitz J, Peled M. Fracture of dental implants; literature review and report of a case. Implant Dent. 2002;1:137–43.
17. Morgan MJ, James DF, Pilliar RM. Fractures of the fixture component of an osseointegrated implant. Int J Oral Maxillofac Implants. 1993;8:409–14.
18. Rangert B, Krogh P, Langer B, Van Roekel N. Bending overload and implant failure: a retrospective clinical analysis. Int J Oral Maxillofac Implants. 1995;10:326–34.
19. Huang HW, Tsai CH, Chang CC, Lin CT, Lee SY. Evaluation of loading conditions on fatigue-failed implants by fracture surface analysis. Int J Oral Maxillofac Implants. 2005;20:854–9.
20. Dittmer MP, Dittmer S, Borchersh L, Kohorst P, Stiesch M. Influence of the interface design on the yield force of the implant-abutment complex before and after cyclic mechanical loading. J Prosthodont Res. 2012;56:19–24.
21. Chan HL, Oh WS, Ong HS, Fu JH, Steigmann M, Sierraalta M, Wang HL. Impact of implantoplasty on strength of the implant-abutment complex. Int J Oral Maxillofac Implants. 2013;28:1530–5.